

H 80-005

Collapse of Turbulent Wakes in Stably Stratified Media

Samuel Hassid*

The Pennsylvania State University, University Park, Pa.

20006
20007

A simple turbulent energy model and a calculation procedure are proposed, which are able to reproduce the main features of the collapse of turbulent wakes behind towed or self-propelled bodies in stratified environments. The predictions of the model are shown to be in good agreement with the detailed experimental data of Lin and Pao, as well as with flow visualization experiments of other workers.

Nomenclature

$A, A', A'', c_1,$	
$c_2, c_{1T}, c_{2T}, c_T,$	
c_{c1}, c_{c2}, σ_t	= constants in the model
c_D	= drag coefficient
D	= body diameter
Fr	= Froude number ($= U_0/DN$)
g	= acceleration due to gravity
g_i	= acceleration due to gravity vector
H	= wake height
k	= turbulent energy per unit volume
N	= Brunt-Väisälä frequency
P	= mean pressure
P_s	= pressure deviation from hydrostatic state
R	= Richardson number ($R^{1/2} = r_0 \sqrt{\beta \alpha g / V_0}$)
Ri	= Richardson number ($= H^2 N^2 / k$)
r_0	= initial radius of mixed region
T	= mean temperature
t_{col}	= time to start of collapse
U^i	= mean velocity vector
U_d	= velocity defect
U_D	= velocity defect at the centerline
U_0	= body velocity
U, V, W	= streamwise, horizontal cross-stream, and vertical cross-stream mean velocity components, respectively
u^i	= fluctuating velocity vector
u, v, w	= streamwise, horizontal cross-stream, and vertical cross-stream fluctuating velocity components, respectively
$\bar{u}, \bar{v}, \bar{w}$	= root-mean-square fluctuating velocity components
W	= wake width
x^i	= position vector
x, y, z	= streamwise, horizontal cross-stream, and vertical cross-stream coordinates, respectively
Z	= wake half-width
$z_{1/2}$	= distance between centerline and point where $k = k(0)/4 \dots$
α	= temperature gradient of undisturbed fluid
β	= volumetric expansion coefficient
ϵ	= turbulent energy dissipation rate per unit volume

θ	= temperature fluctuation
ν_v, ν_w	= eddy diffusivity coefficients for momentum in the horizontal and vertical direction, respectively
ν_{Tv}, ν_{Tw}	= eddy diffusivity coefficients for heat in the horizontal and vertical directions, respectively
ρ	= density
ρ_0	= density at the centerline

Introduction

A TURBULENT wake in a stably stratified fluid exhibits some peculiar features which are not encountered in wakes in nonstratified media. Whereas axisymmetric wakes in homogeneous fluids increase indefinitely in width under the action of the diffusive turbulent forces, wakes in stably stratified environments are known to reach a maximum vertical extent and subsequently collapse to a minimum height. At the same time, under the combined action of turbulent diffusion and gravitational forces, they increase in the horizontal direction faster than they would in a neutral medium. Furthermore, the decrease in the vertical extent is associated with the generation of gravitational internal waves which propagate through the surrounding fluid. (See Fig. 1.)

The first experimental investigation of this phenomenon was conducted by Schooley and Stewart,¹ who used a flow visualization technique to observe the wake behind a self-propelled body. The same flow has since been documented in detail by Stockhausen, Clark, and Kennedy,² Lin and Pao,^{3,4} and Stromm;⁵ Pao and Lin have focused on the wake behind a towed body in a stably stratified medium.^{6,7} Van der Watering, Tulin, and Wu,⁸ Sundaram, et al.,⁹ and Merritt,¹⁰ investigated the collapse of mixed turbulent regions generated by different means in quiescent, stably stratified media. These phenomena are closely related to the decay of momentumless wakes in such media, since turbulence in momentumless wakes is known to behave in a way similar to turbulence behind a point source. Wu¹¹ has observed the collapse of a tube of homogeneous, nonturbulent fluid in a stably stratified environment and the resulting wave pattern.

Theoretical investigations by Wessel¹² and Young and Hirt¹³ focus on the collapse of a nonturbulent fully mixed region. Hartman and Lewis¹⁴ examined analytically the case of a degree of mixing (defined as the ratio of the density gradient inside the mixed region to the ambient density gradient) approximately equal to one, for which a linear analysis can be used. They predict that the initially circular region, after several oscillations, settles to an elliptical shape in equilibrium with the ambient density.

The above flows are different from the collapse of a turbulent mixed region. Theoretical treatments of this problem include the semiempirical models of Ko¹⁵ and Merritt¹⁰ which predict the evolution of the wake height and width of the

Received Dec. 12, 1977; revision received Dec. 3, 1979. Copyright © American Institute of Aeronautics and Astronautics, Inc., 1978. All rights reserved. Reprints of this article may be ordered from AIAA Special Publications, 1290 Avenue of the Americas, New York, N.Y. 10019. Order by Article No. at top of page. Member price \$2.00 each, nonmember, \$3.00 each. **Remittance must accompany order.**

Index categories: Hydrodynamics; Jets, Wakes and Viscid-Inviscid Flow Interactions.

*Research Associate, Applied Research Laboratory.

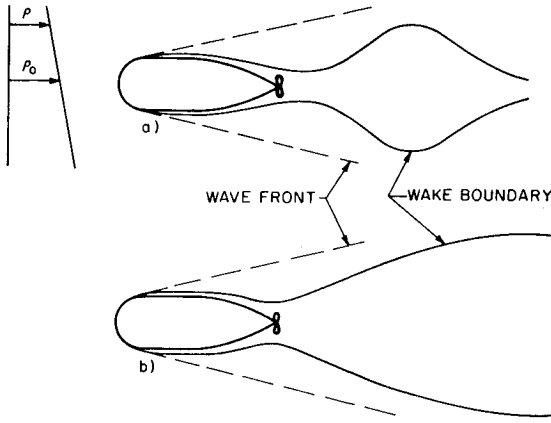


Fig. 1 Wake of a self-propelled body in a stably stratified fluid: a) horizontal view, b) vertical view.

turbulent mixed region in a stably stratified environment. The theoretical treatment of Vasiliev, et al.,¹⁶ is based upon the transport equations for the components of the Reynolds stress tensor and the turbulent heat fluxes. These authors neglect the nonlinear terms in the Navier-Stokes equations. It is doubtful that such an approximation is justified, since these are the very terms that cause the collapse. Furthermore, their model predicts no collapse, but only a slowing down in the growth of the turbulent mixed region. Finally, the model of Lewellen, et al.,¹⁷ is based essentially upon the transport equation for the turbulent energy k coupled with an equation for L , the characteristic length scale of turbulence, which is a measure of the size of the turbulence producing eddies.

In this work it is proposed to use a simple turbulent energy-dissipation ($k-\epsilon$) model, coupled with a computational procedure, which will enable one to describe the collapse of turbulent wakes in stably stratified media and identify the main parameters that influence this phenomenon. The $k-\epsilon$ model has been shown to be preferable to the $k-L$ model, because the ϵ equation contains fewer terms than the L equation and because there is no difficulty in determining a boundary condition for ϵ .

Fundamental Equations

Consider the wake behind a body moving with uniform velocity in a stably stratified medium with uniform temperature (or density) gradient. (The application of the model to salinity stratified media is straightforward.) Assuming the Boussinesq approximation to be valid, i.e., that the specific weight of the fluid is variable but its density can be considered constant, one obtains the following form for the Reynolds equation and the continuity equation

$$U_j \frac{\partial U_i}{\partial x_j} + \frac{1}{\rho} \frac{\partial P}{\partial x_i} = g_i (1 - \beta T) - \frac{\partial}{\partial x_j} \overline{u_i u_j} \quad (1)$$

$$\frac{\partial U_i}{\partial x_i} = 0 \quad (2)$$

Here T is the deviation of the temperature from some reference level, which in this case can be chosen to be the temperature at the centerline of the wake.

In addition the following assumptions will be made: 1) The flow is elliptic in z and y directions, and parabolic in x direction; 2)

$$U_0 \gg U_d \quad (3)$$

where U_0 is the velocity of the body and U_d is the local velocity defect; and 3)

$$|\overline{vw}| \ll \overline{w^2} \quad (4)$$

Thus the equations take the following form

$$U_0 \frac{\partial U_d}{\partial x} + V \frac{\partial U_d}{\partial y} + W \frac{\partial U_d}{\partial z} + \frac{\partial \overline{u^2}}{\partial x} = -\frac{1}{\rho} \frac{\partial P_s}{\partial x} - \frac{\partial \overline{uv}}{\partial y} - \frac{\partial \overline{uw}}{\partial z} \quad (5)$$

$$U_0 \frac{\partial V}{\partial x} + V \frac{\partial V}{\partial y} + W \frac{\partial V}{\partial z} + \frac{\partial \overline{v^2}}{\partial y} = \frac{1}{\rho} \frac{\partial P_s}{\partial y} \quad (6)$$

$$U_0 \frac{\partial W}{\partial x} + V \frac{\partial W}{\partial y} + W \frac{\partial W}{\partial z} + \frac{\partial \overline{w^2}}{\partial z} = -\frac{1}{\rho} \frac{\partial P_s}{\partial z} + \beta g (T - \alpha z) \quad (7)$$

$$\frac{\partial V}{\partial y} + \frac{\partial W}{\partial z} = 0 \quad (8)$$

Here P_s is the deviation of the pressure from the unperturbed hydrostatic pressure, whereas αz is the unperturbed temperature distribution which is assumed to be linear.

Notice that $\partial U_d / \partial x$ has been neglected in the continuity equation (8). In the absence of gravitational forces, such a neglect would not be justified (but then the V and W convective terms in Eqs. (5-7) could be altogether neglected). On the other hand, stratification results in a flow pattern in the y and z direction, whose decay is much slower than that of the streamwise velocity defect U_d , which is affected mainly by turbulent diffusive forces.

By differentiating Eq. (6) with respect to y and Eq. (7) with respect to z and adding, a Poisson equation for the pressure can be obtained:

$$\frac{\partial^2}{\partial y^2} \left(\frac{P_s}{\rho} + \overline{v^2} \right) + \frac{\partial^2}{\partial z^2} \left(\frac{P_s}{\rho} + \overline{w^2} \right) = \beta g \frac{\partial}{\partial z} (T - \alpha z) - S \quad (9)$$

where

$$S = \frac{\partial^2}{\partial y^2} (\overline{V^2}) + \frac{\partial^2}{\partial z^2} (\overline{W^2}) + 2 \frac{\partial^2}{\partial y \partial z} (\overline{VW}) \quad (10)$$

In addition, the following equation governs the transport of temperature:

$$U_0 \frac{\partial T}{\partial x} + V \frac{\partial T}{\partial y} + W \frac{\partial T}{\partial z} = -\frac{\partial}{\partial y} \overline{v\theta} - \frac{\partial}{\partial z} \overline{w\theta} \quad (11)$$

In order to solve the above system of equations, closure approximations are needed for the Reynolds stresses \overline{uv} and \overline{uw} , as well as for the turbulent heat fluxes $\overline{v\theta}$ and $\overline{w\theta}$. These will be discussed in the following section.

Turbulent Flow Model

Recently the Reynolds stress model has become increasingly popular in computational investigations of turbulent flow. For free turbulent flows, however, the simpler $k-\epsilon$ model may give results which are in better agreement with experiment. (See Launder, et al.,¹⁸ and Hassid.¹⁹) Needless to say, of course, that the $k-\epsilon$ model is preferable from the standpoint of computer storage and time requirements.

The closure used here is essentially based on the model of McQuirk and Rodi.²⁰ Transport equations are used for both the turbulent energy k and the dissipation rate ϵ , and gradient diffusion forms for the Reynolds stresses. However, the expressions for the latter quantities are derived from invariant second-order models by neglecting the advection and turbulent transport terms.

The expressions for $\overline{u_i u_j}$ and $\overline{u_i \theta}$ are

$$\frac{\overline{u_i u_j}}{k} = \frac{(1 - c_2)}{c_1} \frac{\Pi_{ij}}{\epsilon} - \frac{2}{3} \frac{(1 - c_1 - c_2)}{c_1} \delta_{ij} \quad (12)$$

where

$$\Pi_{ij} = - \left(\overline{u_i u_k} \frac{\partial U_j}{\partial x_k} + \overline{u_j u_k} \frac{\partial U_i}{\partial x_k} \right) - \beta (g_i \overline{u_j \theta} + g_j \overline{u_i \theta}) \quad (13)$$

$$\overline{u_i \theta} = - \frac{k}{c_{IT} \epsilon} \left[\overline{u_i u_k} \frac{\partial T}{\partial x_k} + (1 - c_{2T}) \left(\overline{u_k \theta} \frac{\partial U_i}{\partial x_k} + \beta g_i \overline{\theta^2} \right) \right] \quad (14)$$

$\overline{\theta^2}$ is calculated assuming equilibrium between production and dissipation of this quantity. It is assumed that the rate of destruction of the temperature variance $\overline{\theta^2}$ is also proportional to the mechanical dissipation

$$\overline{\theta^2} = - \frac{2}{c_T} \frac{k}{\epsilon} \overline{u_j \theta} \frac{\partial T}{\partial x_j} \quad (15)$$

McGuirk and Rodi used their model to describe jet flows in stratified media. Wake flows differ from jet flows in that the latter are parabolic in the y direction. Therefore, in our case, some further approximations are needed. As already stated, $\overline{v w}$ will be neglected in comparison with the normal Reynolds stress components. Thus, the equations for the turbulent heat fluxes are

$$-\overline{u \theta} = \frac{k}{c_{IT} \epsilon} \left[\overline{u w} \frac{\partial T}{\partial z} + \overline{u v} \frac{\partial T}{\partial y} + (1 - c_{2T}) \left(\overline{w \theta} \frac{\partial U}{\partial z} + \overline{v \theta} \frac{\partial U}{\partial y} \right) \right] \quad (16)$$

$$-\overline{v \theta} = \frac{k}{c_{IT} \epsilon} \frac{\overline{v^2}}{v^2} \frac{\partial T}{\partial y} \quad (17)$$

$$-\overline{w \theta} = \frac{k}{c_{IT} \epsilon} \left[\overline{w^2} \frac{\partial T}{\partial z} - (1 - c_{2T}) \beta g \overline{\theta^2} \right] \quad (18)$$

In order to eliminate $\overline{\theta^2}$ in the above equations, it will be further assumed that the production of $\overline{\theta^2}$ by the horizontal temperature gradient $\partial T / \partial y$ is small compared to the production by the vertical gradient $\partial T / \partial z$. Thus Eq. (15) becomes

$$\overline{\theta^2} = - \frac{2}{c_T} \frac{k}{\epsilon} \overline{w \theta} \frac{\partial T}{\partial z} \quad (19)$$

This assumption is valid only for the far wake region where the buoyant forces are important. In this region, $\partial T / \partial y$ decays because of the spreading of the wake, whereas $\partial T / \partial z$ remains constant. It is not justified in the near wake in which diffusional forces are significant. In this region, however, the effect of this assumption on $\overline{w \theta}$ is small.

Substituting Eq. (19) into Eq. (18)

$$-\overline{w \theta} = \frac{(k \overline{w^2} / c_{IT} \epsilon) (\partial T / \partial z)}{1 + [2(1 - c_{2T}) / c_T] (k^2 / \epsilon^2) \beta g (\partial T / \partial z)} \quad (20)$$

Now, from Eq. (12), one obtains the following expressions for $\overline{v v}$ and $\overline{w w}$

$$\overline{v^2} = - \frac{2}{3} \frac{(1 - c_l - c_2)}{c_l} k \quad (21)$$

$$\overline{w^2} = - \frac{2}{3} \frac{(1 - c_l - c_2)}{c_l} k + 2 \frac{(1 - c_2)}{c_l} \beta g \frac{k}{\epsilon} \overline{w \theta} \quad (22)$$

Substituting into Eqs. (17) and (20)

$$-\overline{v \theta} = \nu_{Tv} \frac{\partial T}{\partial y} = c_\theta \frac{k^2}{\epsilon} \frac{\partial T}{\partial y} \quad (23)$$

$$-\overline{w \theta} = \nu_{Tw} \frac{\partial T}{\partial z} = \frac{c_\theta (k^2 / \epsilon) (\partial T / \partial z)}{1 + A (k^2 / \epsilon^2) \beta g (\partial T / \partial z)} \quad (24)$$

where

$$c_\theta = - \frac{2}{3} [(1 - c_l - c_2) / c_l c_{IT}] \quad (25)$$

and

$$A = (2 / c_{IT}) [(1 - c_{2T}) / c_T + (1 - c_2) / c_l] \quad (26)$$

Turning to the equations for the Reynolds stress

$$\overline{u v} = - \frac{1 - c_2}{c_l} \frac{k \overline{v^2}}{\epsilon} \frac{\partial U}{\partial y} \quad (27)$$

$$\overline{u w} = - [(1 - c_2) / c_l] [(k \overline{w^2} / \epsilon) (\partial U / \partial z) - \beta g \overline{u \theta}] \quad (28)$$

Again, using Eqs. (21) and (27)

$$-\overline{u v} = \nu_v \frac{\partial U}{\partial y} = c_M \frac{k^2}{\epsilon} \frac{\partial U}{\partial y} \quad (29)$$

where

$$c_M = - \frac{2}{3} [(1 - c_2) / c_l] [(1 - c_l - c_2) / c_l] \quad (30)$$

Neglecting, as already mentioned, $\partial T / \partial y$ in the equation for $\overline{u \theta}$ and substituting in Eq. (28), one ends with

$$-\overline{u w} = \nu_w \frac{\partial U}{\partial z} = c_M \frac{k^2}{\epsilon} \frac{(1 + A' F)}{(1 + A'' F)(1 + A F)} \frac{\partial U}{\partial z} \quad (31)$$

where

$$F = \beta g \frac{k^2}{\epsilon^2} \frac{\partial T}{\partial z} \quad (32)$$

and

$$A' = A - \left(2 \frac{1 - c_2}{c_l} + \frac{1 - c_{2T}}{c_{IT}} \right) \frac{1}{c_{IT}} \quad (33a)$$

$$A'' = (1 - c_2) / (c_{IT} c_l) \quad (33b)$$

As already mentioned, k and ϵ are calculated from the relevant transport equations:

$$U_0 \frac{\partial k}{\partial x} + V \frac{\partial k}{\partial y} + W \frac{\partial k}{\partial z} = \frac{\partial}{\partial y} \left(\nu_v \frac{\partial k}{\partial y} \right) + \frac{\partial}{\partial z} \left(\nu_w \frac{\partial k}{\partial z} \right) + \nu_v \left(\frac{\partial U}{\partial y} \right)^2 + \nu_w \left(\frac{\partial U}{\partial z} \right)^2 + \beta g \overline{w \theta} - \epsilon \quad (34)$$

$$U_0 \frac{\partial \epsilon}{\partial x} + W \frac{\partial \epsilon}{\partial y} + W \frac{\partial \epsilon}{\partial z} = \frac{\partial}{\partial y} \left(\frac{\nu_v}{\sigma_\epsilon} \frac{\partial \epsilon}{\partial y} \right) + \frac{\partial}{\partial z} \left(\frac{\nu_w}{\sigma_\epsilon} \frac{\partial \epsilon}{\partial z} \right) - c_{\epsilon 2} \frac{\epsilon^2}{k} + c_{\epsilon 1} \frac{\epsilon}{k} \left[\nu_v \left(\frac{\partial U}{\partial y} \right)^2 + \nu_w \left(\frac{\partial U}{\partial z} \right)^2 + \beta g \overline{w \theta} \right] \quad (35)$$

Here the model differs from the one of McGuirk and Rodi because they claim that gravitational production should not appear in the equation for ϵ . It was found that such an assumption leads to unrealistically low values for k . It should be mentioned that there is wide disagreement among different research groups on the question of the influence of buoyant forces on the ϵ equation.

The constants used are:

$$\begin{array}{llll} c_1 = 2.2 & c_{\epsilon 1} = 1.44 & \sigma_{\epsilon} = 1.3 & c_{2T} = 0.5 \\ c_2 = 0.55 & c_{\epsilon 2} = 1.92 & c_{1T} = 3.2 & c_T = 1.25 \end{array}$$

Out of all the approximations used, the neglect of $\partial T / \partial y$ which was necessary in order to obtain the gradient forms for the Reynolds stress equations, is the one likely to cause the greatest error. Notice, however, that for the nonbuoyant case, the expressions derived above are exact.

Method of Solution

The system of equations to be solved consists of the momentum equation for U_d and V

$$\begin{aligned} U_0 \frac{\partial U_d}{\partial x} + V \frac{\partial U_d}{\partial y} + W \frac{\partial U_d}{\partial z} + \frac{\partial}{\partial x} \left(\frac{P_s}{\rho} + \overline{v^2} \right) + \frac{\partial}{\partial x} (\overline{u^2} - \overline{v^2}) \\ = \frac{\partial}{\partial y} \left(\nu_v \frac{\partial U_d}{\partial y} \right) + \frac{\partial}{\partial z} \left(\nu_w \frac{\partial U_d}{\partial z} \right) \end{aligned} \quad (36)$$

$$U_0 \frac{\partial V}{\partial x} + V \frac{\partial V}{\partial y} + W \frac{\partial V}{\partial z} + \frac{\partial}{\partial y} \left(\frac{P_s}{\rho} + \overline{v^2} \right) = 0 \quad (37)$$

The transport equation for temperature

$$U_0 \frac{\partial T}{\partial x} + V \frac{\partial T}{\partial y} + W \frac{\partial T}{\partial z} = \frac{\partial}{\partial y} \left(\nu_{Tv} \frac{\partial T}{\partial y} \right) + \frac{\partial}{\partial z} \left(\nu_{Tw} \frac{\partial T}{\partial z} \right) \quad (38)$$

The Poisson equation for pressure

$$\begin{aligned} \frac{\partial^2}{\partial y^2} \left(\frac{P_s}{\rho} + \overline{v^2} \right) + \frac{\partial^2}{\partial z^2} \left(\frac{P_s}{\rho} + \overline{v^2} \right) + \frac{\partial^2}{\partial z^2} (\overline{w^2} - \overline{v^2}) \\ = \beta g \frac{\partial}{\partial z} (T - \alpha z) - S \end{aligned} \quad (39)$$

where S is given by Eq. (10), the continuity equation (8), the transport equations for the turbulent energy k [Eq. (34)], and the dissipation rate ϵ [Eq. (35)]. In addition, the following expressions for $\overline{u^2} - \overline{v^2}$ and $\overline{w^2} - \overline{v^2}$ can be derived from Eq. (12)

$$\overline{u^2} - \overline{v^2} = - \frac{(1 - c_2)}{c_1} \left(\overline{uv} \frac{\partial U_d}{\partial y} + \overline{uw} \frac{\partial U_d}{\partial z} \right) \quad (40)$$

$$\overline{w^2} - \overline{v^2} = \frac{2(1 - c_2)}{c_1} \beta g \frac{k}{\epsilon} \overline{w\theta} \quad (41)$$

This system was converted into a set of difference equations. Forward differencing was used in the x direction, centered differencing for the diffusive terms, and upwind differencing for the lateral transport terms. The use of upwind differencing can result in artificial viscosity errors, which, however, do not affect appreciably the main features of the flow, such as the predicted development of maximum turbulent energy, velocity defect, and wake dimensions. In the nonstratified case, when the flow is axisymmetrical, the error in these quantities is on the order of 10% for the length scale and turbulent energy and 15% for the velocity defect. For the case of strong stratification, doubling the mesh points results in changes on the order of 10%.

The mesh system used (Fig. 2) consists of an inner mesh AEFG in which the turbulent processes occur and an outer mesh in which there is no turbulence. The outer mesh was three times as large as the inner mesh. The reason is that both experimental evidence and computer calculations suggest that the waves caused by the collapse of a nonturbulent mixed region advance twice the original width of that region after two Brunt-Väisälä periods. Since there are very few ex-

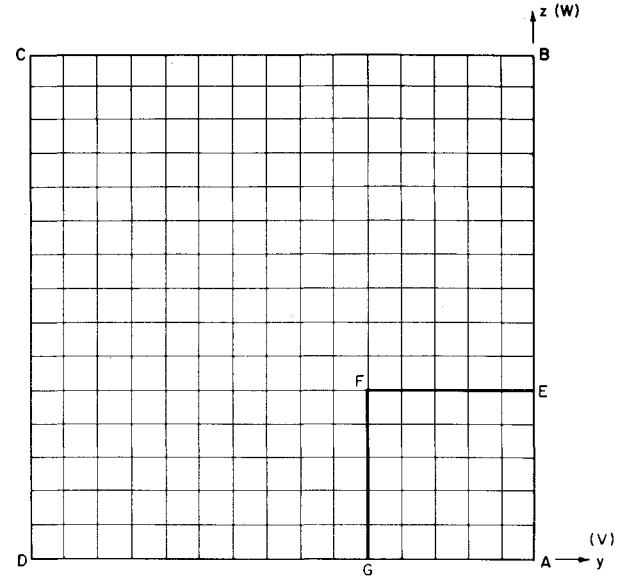


Fig. 2 Mesh system, first quadrant.

perimental data for times larger than two Brunt-Väisälä periods and since the wave phenomena are much weaker when the mixed region is turbulent, this mesh was estimated to be adequate.

The mesh used was allowed to expand, so that the original growth due to turbulent diffusion can be simulated.

The following boundary conditions were used:

On AB

$$V = \frac{\partial W}{\partial y} = \frac{\partial}{\partial y} \left(\frac{P_s}{\rho} + \overline{v^2} \right) = \frac{\partial U_d}{\partial y} = 0 \quad (42)$$

On AD

$$\frac{\partial V}{\partial z} = W = \frac{\partial}{\partial z} \left(\frac{P_s}{\rho} + \overline{v^2} \right) = \frac{\partial U_d}{\partial z} = 0 \quad (43)$$

On BC

$$V = \frac{\partial W}{\partial z} = P_s = U_d = 0 \quad (44)$$

On CD

$$\frac{\partial V}{\partial y} = W = P_s = U_d = 0 \quad (45)$$

For k and ϵ , the boundary conditions were

On EF and FB

$$k = \epsilon = 0 \quad (46)$$

On AE

$$\frac{\partial k}{\partial y} = \frac{\partial \epsilon}{\partial y} = 0 \quad (47)$$

On AG

$$\frac{\partial k}{\partial z} = \frac{\partial \epsilon}{\partial z} = 0 \quad (48)$$

Admittedly, the conditions on V , W , and P_s at the outer boundaries BC and CD are artificial and will result in wave reflection. However, since the characteristic wavelength of the waves generated by the collapse is expected to be of the order of one wake height or width and since the characteristic time

is the Brunt-Väisälä period, it is estimated that these boundary conditions will not cause large errors for times less than two Brunt-Väisälä periods, i.e., the time taken by the wavefront to reach the external boundaries. As a check, the differential equations were solved using different boundary conditions on BC and CD and this did not significantly affect the results in the turbulent region.

Results and Comparison with Experiment

The main scaling parameter used by most investigators^{3,6,8-10} for wake flows in stratified media is the Froude number, defined as

$$Fr = U_0 / ND \quad (49)$$

where N is the Brunt-Väisälä frequency

$$N = \frac{1}{2\pi} \left(-\frac{g}{\rho} \frac{\partial \rho}{\partial z} \right)^{1/2} \quad (50)$$

This scaling factor is suitable only for wakes. In general, the extent that a mixed region will grow before collapsing is determined rather by the Richardson number, which expresses the ratio between the potential energy and the turbulent kinetic energy at the origin

$$Ri = H^2 N^2 / k_0 \quad (51)$$

The development of an initially self-similar momentumless wake in a stratified fluid is shown in Fig. 3a, where the wake height and wake width are compared with the results of Lin

and Pao.³ The wake height and width are taken equal to $2z_{1/2}$ and $2y_{1/2}$, respectively, these values being given by Lin and Pao.⁴ (In our computations, H and W are actually approximately equal to $2.16 z_{1/2}$ and $2.16 y_{1/2}$, respectively.)

The collapse is shown to start at $Nx/U_0 \approx 1/3$. After reaching a maximum height, the wake decreases by about 10% and then increases slightly in the vertical direction. Agreement between the predicted and measured results is generally good. Discrepancies between the experimental data and the predicted width and height are mainly due to the initial profiles, which were assumed to be self-similar. At low Froude numbers, the wake has no time to become self-similar before stratification effects become important. Note, also, that Lin and Pao concede that there is considerable difficulty in measuring the wake height, because of the irregular, fluctuating nature of the outer boundary.

In Fig. 3b, the development, in the vertical and horizontal directions, of an initially self-similar drag wake in a stratified medium is shown. The computed values of $2z_{1/2}$ and $2y_{1/2}$ are compared with the values of H and W measured by Pao and Lin,⁶ because Pao and Lin⁷ claim that for drag wakes $H = 2z_{1/2}$. (In our computations, $H = 2.4z_{1/2}$.)

It is seen that in drag wakes the first maximum is reached at a higher value of Nt than in momentumless wakes and that the reduction in wake height after collapse is smaller. Again, in spite of the influence of stratification on the initial wake dimensions in the experimental errors of flow visualization, the agreement can be considered satisfactory.

In Figs. 4-6, the predicted development of a momentumless and a drag wake in a strongly stratified environment is compared with the experimental data of Lin and Pao⁴ and Pao and Lin.⁷ The following initial conditions were used:

For the momentumless wake

$$k = k_0 \exp(-4r^2/D^2)$$

$$\epsilon = \sqrt{12} (k_0^{3/2}/D) \exp(-6r^2/D^2)$$

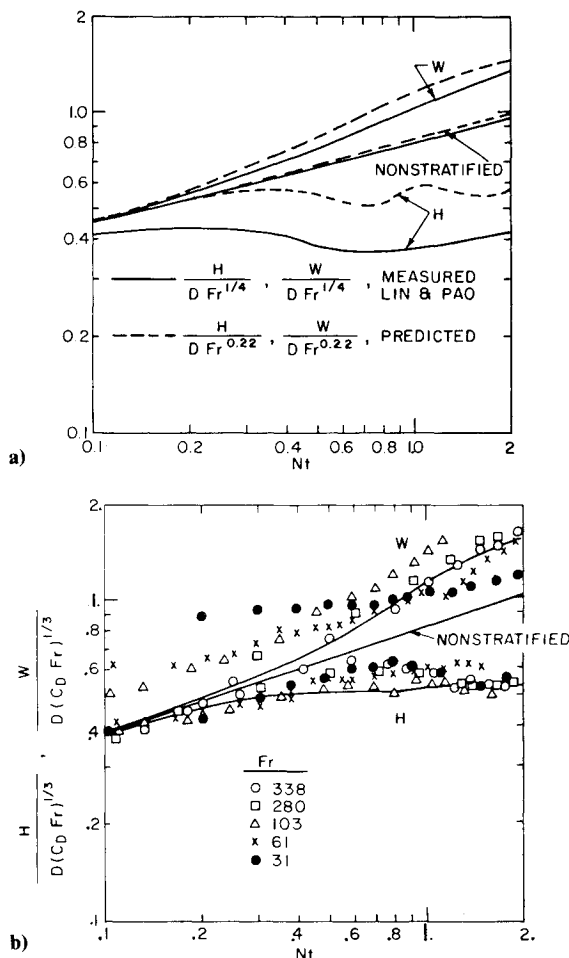


Fig. 3 Nondimensional width and height of a wake in stratified and nonstratified media. a) momentumless wake, data of Lin and Pao;³ b) drag wake, data of Pao and Lin.⁶

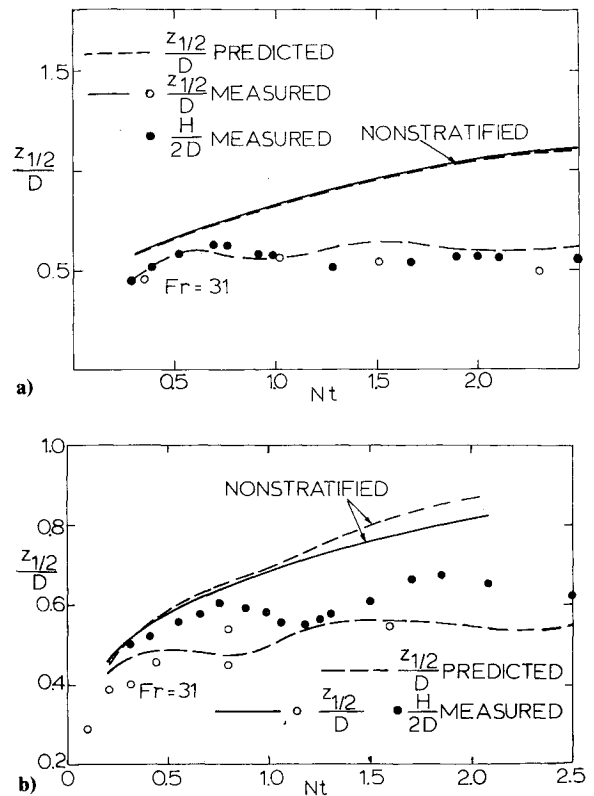


Fig. 4 Height of wakes in stratified and nonstratified media. a) momentumless wake, data of Lin and Pao;⁴ b) drag wake, data of Pao and Lin.⁷

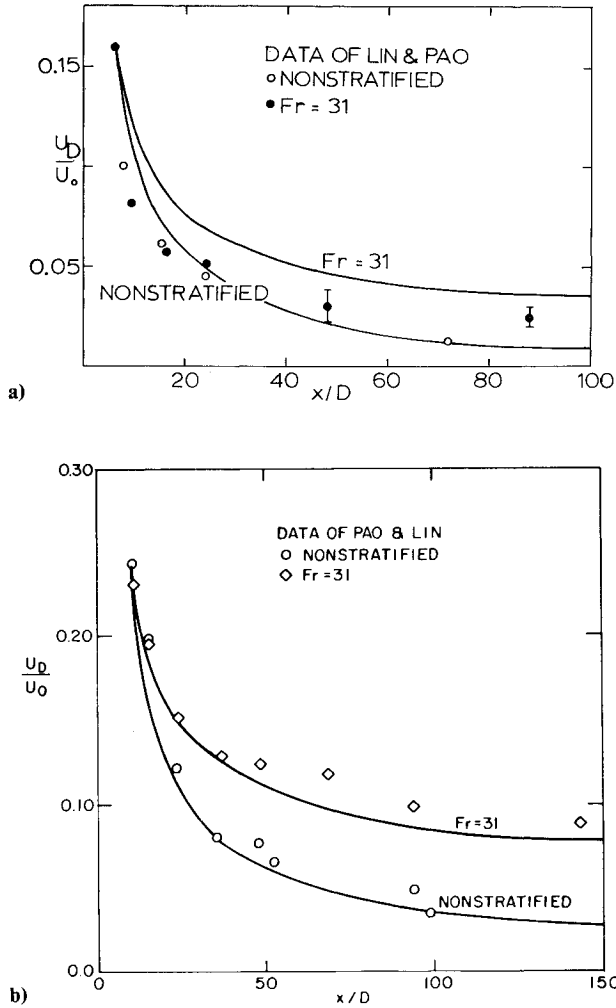


Fig. 5 Centerline velocity defect in wakes in stratified and non-stratified media. a) momentumless wakes, data of Lin and Pao;⁴ b) drag wakes, data of Pao and Lin.⁷

$$U_d = U_{D0} (1 - 8r^2/D^2) \exp(-4r^2/D^2)$$

$$T = \alpha z [1 + \exp(-4r^2/D^2)] \quad (52)$$

For the drag wake

$$k = k_0 \exp(-r^2/A)$$

$$\epsilon = \sqrt{3/A} k_0^{3/2} \exp(-3r^2/2A)$$

$$U_d = U_{D0} \exp(-r^2/A)$$

$$T = \alpha z [1 + \exp(-r^2/A)] \quad (53)$$

where

$$A = c_D D^2 U_0 / 8 U_{D0} \quad (54)$$

U_{D0} and k_0 are the initial values of the velocity centerline defect and the turbulent energy, respectively. Note that V and W were taken initially equal to zero throughout the flowfield.

In Fig. 4, the predicted wake height is compared with the results of Lin and Pao⁴ and Pao and Lin.⁷ The system of maximums and minimums is well reproduced, with a certain phase difference due to the use of $V=0$ and $W=0$ as initial conditions.

In Fig. 5, it is seen that stratification results in slower decay of the velocity defect, for both drag wakes and momentumless wakes. Agreement with the experimental data is very good.

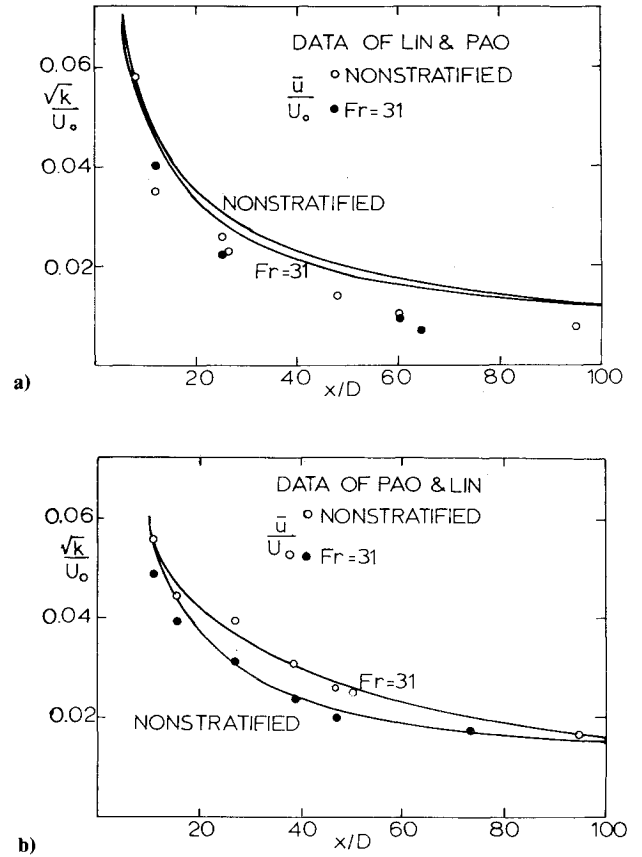


Fig. 6 Centerline turbulent energy in wakes in stratified and non-stratified media. a) momentumless wakes, data of Lin and Pao;⁴ b) drag wakes, data of Pao and Lin.⁷

In Fig. 6, the decay of turbulent energy with and without stratification is shown. Since in Refs. 4 and 7 only the axial velocity fluctuation (\bar{u}) is given and since the $k-\epsilon$ model can predict only the total turbulent energy k , the measured value of \bar{u} is compared with the predicted value of \sqrt{k} . These two quantities are not, of course, the same. However, since \bar{u} is the largest component of the turbulent energy, the trends in the two quantities are similar. It is seen that in spite of the additional sink term in the turbulent energy equation, expressing the conversion of turbulent kinetic energy into potential energy, the difference in the turbulence levels is very small, especially in the momentumless wake. Though the predicted \sqrt{k} is compared with the measured value of \bar{u} , agreement between theory and experiment is very good.

Finally in Table 1 the predicted values of the maximum and minimum heights as well as the collapse times of mixed regions and momentumless wakes are compared with their values, as measured by several experimental workers.^{1,2,8-10}

In Table 1, t_{col} is the time (for mixed regions; distance divided by mean body velocity in momentumless wakes) at which the wake reaches the first maximum height, H_{max} and H_{min} are the first maximum and minimum wake heights, respectively, whereas the Richardson number R is defined as

$$R^{1/2} = \frac{r_0 \sqrt{\beta \alpha g}}{dZ/dt} \quad (55)$$

where dZ/dt is the initial rate of spreading of the mixed region and r_0 is the initial radius. (For the experiments of Schooley and Stewart, Stockhausen, et al., and Merritt, r_0 is the body diameter.) In the case of Van der Watering, et al., the initial rate of spreading was given by the authors, whereas in the other experiments this quantity had to be estimated from the data. Also note that Merritt conducted experiments with

Table 1 Collapse time, maximum height, and minimum height of turbulent mixed regions in stably stratified media

Reference		Nt_{col}		H_{max}/r_0		H_{min}/r_0	
		Measured	Predicted	Measured	Predicted	Measured	Predicted
Schooley and Stewart ¹	$Fr = 60$	0.337	0.287	2.16	2.00	1.36	1.80
Stockhausen, Clark, and Kennedy ²	$Fr = 100$	0.260	0.191	3.00	2.08	2.10	1.80
Merritt ¹⁰	$Fr = 100$	0.300	0.191	3.00	2.08	1.80	1.80
Van der Watering, Tulin, and Wu ⁸	$R^{1/2} = 1.34$	0.215	0.146	1.51	1.26	1.11	0.96
	1.56	0.236	0.156	1.25	1.23	1.04	0.91
	1.56	0.192	0.156	1.31	1.26	1.06	0.93
	2.19	0.215	0.144	1.11	1.17	0.90	0.80
	2.19	0.215	0.145	1.19	1.17	0.90	0.82
	3.09	0.223	0.125	1.06	1.09	...	0.68
	4.23	0.195	0.081	0.95	1.03	0.77	0.57
	4.27	0.167	0.111	1.00	1.05	0.83	0.62
	1.56	0.178	0.148	1.24	1.20	0.94	0.86
	1.57	0.178	0.150	1.25	1.21	0.89	0.87
	2.28	0.142	0.121	1.20	1.13	1.00	0.72
	3.21	0.198	0.148	1.13	1.13	0.94	0.63
	2.06	0.167	0.103	1.20	1.06	1.03	0.63
	1.89	0.116	0.111	1.04	1.07	0.88	0.65
	3.69	0.170	0.080	1.04	1.09	...	0.58
	5.21	0.204	0.093	0.88	1.04	0.77	0.59
	5.29	0.188	0.072	0.95	1.02	0.88	0.55
Sundaram, Stratton, and Rehm ⁹	3.20	0.595	0.115	1.54	1.12	1.07	0.71
	2.80	0.382	0.119	1.31	1.13	1.00	0.74

many Froude numbers, but only the case of $Fr = 100$ is fully documented in Ref. 10.

There are, of course, many sources of error in this table. Since no initial turbulent energy and dissipation profiles were available, the initial turbulent energy and dissipation profiles were assumed to be self-similar and the initial turbulent energy was deduced from the initial rate of spread through the relation

$$\frac{1}{\sqrt{k}} \frac{dZ}{dt} = 0.26 \quad (56)$$

which is applicable to self-similar flow in nonstratified media. Given, however, the very high Richardson numbers, it is very unlikely that the turbulent energy distribution will reach self-similarity. The initial temperature (density) profile was assumed to be fully mixed in the turbulent region. The predicted value of t_{col} is the value of t when the vertical extent of the mixed region starts decreasing. Typically, however, the mixed region may decrease by less than 5% at $t = 2t_{col}$ and it is only then that it can be observable in a flow visualization experiment.

Finally, it should be stated that the experiments quoted in Table 1 are widely different from each other. The first two authors experimented with moving bodies, and the last three with mixed turbulent regions induced in different ways. In the former two experiments, the production of turbulent energy by mean velocity gradients could not be taken into account.

In spite of all these considerations and in view of the crudeness of the observation methods, the numerous assumptions needed for the calculation, and the differences among the data, the amount of agreement exhibited in Table 1 is encouraging.

Discussion and Conclusions

The development of momentumless wakes, drag wakes, and turbulent regions in stably stratified media was investigated using a simple turbulent energy-dissipation model. This is the simplest turbulent flow model that can be used for

such flows; evidence from calculations in nonstratified media suggests that for wake flows, this model is also more accurate than the more sophisticated Reynolds stress models.

The effect of stratification is expressed through a damping factor in the eddy diffusivity coefficients for vertical exchange of momentum and heat. The eddy diffusivities in the horizontal direction remain unaffected.

As a result of turbulent mixing, the density in the wake is different from the ambient density. The fluid is heavier than the surroundings above the horizontal symmetry plane and lighter below that plane. Thus, diffusive expansion in the vertical direction is opposed by buoyancy forces. On the other hand, the buoyancy forces increase the rate of expansion of the wake width in the horizontal direction.

The decay of the wake can be divided into two regions:

1) The expansion region in which the wake expands in all directions at approximately the same rate under the influence of the turbulent diffusive forces. For flows with relatively weak stratification (high Froude number or low Richardson number), this region extends to $Nx/U_0 = 1/3$ for momentumless wakes and $Nx/U_0 = 2/5$ for drag wakes. At these points the wake height reaches a maximum. Wide variations from these limits are possible, depending upon the initial turbulence level and the initial potential energy, which is a function of the initial density deviation from the ambient density distribution. In this region, the diffusive turbulent forces are stronger than the gravitational forces.

2) The collapse region in which the gravitational forces become stronger than the diffusional forces, resulting in a reduction in the wake height. The extent of the contraction, however, is small compared to that of fully mixed non-turbulent regions under the same ambient conditions. Whereas the turbulent region contracts by about 10-20%, depending upon the initial conditions, fully turbulent regions diminish indefinitely in height. The reason is that the deviation of the density from its equilibrium distribution is small and decreases continuously under the influence of both diffusion and buoyancy forces.

The initial contraction of the wake is followed by a system of minimums and maximums in the wake height, which result

from the conversion of kinetic into potential energy and vice versa.

The effect of the gravitational forces on the turbulent energy is interesting. In the initial stage, the gravitational forces act as a sink term in the turbulent energy equation and result in lower levels of turbulent energy, relative to what they would have been without stratification. These forces act mainly by converting the vertical component of turbulent energy into potential energy, but affect the other components as well through the mechanism of redistribution of turbulent energy among the different components due to pressure fluctuations.

This effect, however, is balanced by reduced diffusion in the vertical direction. Thus, for $Nx/U_0 > 1$, turbulent energy is almost equal with and without stratification.

The reduced momentum exchange rate in the vertical direction results in a slower decay of the mean velocity defect. It seems as though the centerline velocity defect tends to a constant value, but neither the method nor the data can confirm this trend far downstream. The velocity defect is higher in drag wakes than in momentumless wakes, but this is probably due to the initial conditions.

In summary, one may say that the wake structure subsists much longer in stratified media than in homogeneous media.

The models of Ko and Merritt predict a very large reduction in wake height, of the order of 45% at about one Brunt-Väisälä period. However, Merritt concedes that the degree of mixing at the onset of collapse is of the order of 90%, which would justify a decrease in height slightly higher than 10%, enough to bring the wake in equilibrium with the surroundings. Merritt's method is successful in reproducing several sets of experimental data, mainly of flows where the initial potential energy is high.

The results of Lewellen, et al., are generally similar to the ones predicted in this work. Nevertheless, the approximations used in this work, which result in gradient forms for the Reynolds stress and the turbulent heat fluxes, make the model simpler and result in lower computer storage and time requirements.

The model has, however, several limitations. It is not known whether it can account for the laminarization, that Lin and Pao report occurring after four Brunt-Väisälä periods. The influence of the negative production of turbulent energy on the dissipation equation is not certain and the particular assumption used in this model is only a tentative one, to be modified when a more realistic model is available. The calculation procedure is not reliable for times larger than two Brunt-Väisälä periods, because at such times the artificially imposed boundary conditions may result in reflection of the waves generated by the collapse. In order to overcome this drawback, one may introduce a region of high viscosity in the outer part of the flow, so that the waves are damped before they can be reflected. If this is done, one may obtain a more reliable pattern for the wave motions caused by the collapse, but the computer requirements in time and storage would be significantly increased.

Acknowledgments

This work was sponsored by the Naval Sea Systems Command, Code NSEA-03133, and in part by the Fluid Dynamics Branch, Office of Naval Research.

References

- ¹Schooley, A. H. and Stewart, R. W., "Experiments with a Self-Propelled Body Submerged in a Fluid with Vertical Density Gradient," *Journal of Fluid Mechanics*, Vol. 15, Jan. 1963, pp. 83-96.
- ²Stockhausen, P. J., Clark, C. B., and Kennedy, J. F., "Three Dimensional Momentumless Wakes in Density Stratified Fluids," Dept. of Civil Engineering, Massachusetts Institute of Technology, Rept. 93, June 1966.
- ³Lin, J. T. and Pao, Y. H., "Wakes in Stratified Fluids," *Annual Review of Fluid Mechanics*, Vol. 11, 1979, pp. 317-338.
- ⁴Lin, J. T. and Pao, Y. H., "Velocity and Density Measurements in the Turbulent Wake of a Propeller-Driven Slender Body in a Stratified Fluid," Flow Research Inc., Rept. 36, Aug. 1974.
- ⁵Strom, G. H., "Wind Tunnel Experiments on Wakes in Stratified Flow Including Modeling Criteria and Development of Experimental Equipment," Dept. of Aerospace Engineering and Applied Mechanics, Polytechnic Institute of New York, Rept. 76-11, June 1976.
- ⁶Pao, Y. H. and Lin, J. T., "Turbulent Wake of a Towed Slender Body in Stratified and Nonstratified Fluids: Analysis and Flow Visualizations," Flow Research Inc., Rept. 10, June 1973.
- ⁷Pao, Y. H. and Lin, J. T., "Velocity and Density Measurements in the Turbulent Wake of a Towed Slender Body in Stratified and Nonstratified Fluids," Flow Research Inc., Rept. 12, Dec. 1973.
- ⁸Van der Watering, W. P. M., Tulin, M. P., and Wu, J., "Experiments on Turbulent Wakes in a Stable Density-Stratified Environment," Hydronautics, Inc., TR 231-24, Feb. 1969.
- ⁹Sundaram, T. R., Straton, J. E., and Rehm, R. C., "Turbulent Wakes in a Stratified Medium," Cornell Aeronautical Lab., Rept. AG-3018-A-1, Nov. 1971.
- ¹⁰Merritt, C. E., "Wake Growth and Collapse in Stratified Flow," *AIAA Journal*, Vol. 12, July 1974, pp. 940-949.
- ¹¹Wu, J., "Mixed Region Collapse with Internal Wave Generation in a Density-Stratified Medium," *Journal of Fluid Mechanics*, Vol. 35, Feb. 1969, pp. 531-544.
- ¹²Wessel, W. R., "Numerical Study of the Collapse of a Perturbation in an Infinite Density Stratified Fluid," *Physics of Fluids*, Vol. 12, Dec. 1969, pp. 171-176.
- ¹³Young, J. A. and Hirt, C. W., "Numerical Calculation of Internal Wave Motions," *Journal of Fluid Mechanics*, Vol. 56, Nov. 1972, pp. 265-276.
- ¹⁴Hartmann, R. J. and Lewis, H. W., "Wake Collapse in a Stratified Fluid: a Linear Treatment," *Journal of Fluid Mechanics*, Vol. 51, 1972, pp. 613-618.
- ¹⁵Ko, D. R. S., "A Phenomenological Model for the Momentumless Wake in a Stratified Medium," TRW Rept. 20086-6007-RU00, April 1973.
- ¹⁶Vasiliev, O. F., Kuznetsov, B. G., Lytkin, Y. N., and Chernykh, G. C., "Development of the Turbulent Mixed Region in a Stratified Medium," *Heat Transfer and Turbulent Buoyant Convection*, Vol. I, Spalding, D. B. and Afgan, N., eds., Hemisphere Publishing Corp., Washington, D.C., 1977, pp. 123-138.
- ¹⁷Lewellen, W. S., Teske, M., and Donaldson, Coleman, du P., "Turbulent Wakes in a Stratified Fluid," ARAP 226, Aug. 1974.
- ¹⁸Launder, B. E., Morse, A., Rodi, W., and Spalding, D. B., "A Comparison of the Performance of Six Turbulence Models," Vol. I, *Free Turbulent Shear Flows*, NASA, 1973, pp. 361-426.
- ¹⁹Hassid, S., "Similarity and Decay Laws in Momentumless Wakes," *Physics of Fluids*, to be published. Also, Applied Research Laboratory, Pennsylvania State University, Tech. Memo., File 77-187, May 1977, to be published.
- ²⁰McGuirk, J. J. and Rodi, W., "Calculations of Three Dimensional Heated Surface Jets," *Heat Transfer and Turbulent Buoyant Convection*, Vol. I, Spalding, D. B., and Afgan, N., eds., Hemisphere Publishing Corp., Washington, 1977, pp. 275-287.